Biomedical Research 2019; 30 (4) *ISSN 0970-938X*
www.biomedres.info

Fractal dimension analysis as a discriminant of erythrocytes abnormalities.

Mohamed A. Elblbesy[1,2*]

[1]Department of Medical Laboratory Technology, University of Tabuk, Saudi Arabia

[2]Department of Medical Biophysics, Medical Research Institute, Alexandria University, Egypt

Abstract

This research has evaluated the fractal dimensions of erythrocytes with different morphological characteristics. Predictive function based on fractal dimensions of erythrocytes was constructed to use it in erythrocytes classification. Discriminant analysis was used in the linear combination of computed fractal dimensions of different categories of erythrocytes. Three types of fractal dimensions were calculated for three groups of erythrocytes normal (erythrocyte, echinocyte and sickle cells). There was a significant difference between the fractal dimensions of the three groups. The computed fractal dimensions were used to build the predictive function. The predictive function was highly sensitive and specific in erythrocytes classification. The suggested analytical method may help in the transformation of blood smear observation to a fully automated process. Hence it can reduce the errors and improve the accuracy of such medical diagnosis methods.

Keywords: Fractal, Dimension, Erythrocytes, Discriminant.

Accepted on January 18, 2018

Introduction

The applicability of fractal geometry to further understanding of diverse phenomena has proliferated since Benoit Mandelbrot's seminal work in the 1970s. The works of Mandelbrot and Nottale inspired the development of fractal physics [1]. Fractals are a rough, complex geometric shape that can be subdivided into parts. Fractal geometric analysis is used in quantification and discrimination between different types of fractal objects. The fractals can be described using fractal measure (K) and fractal dimension (FD) [2-9]. Fractal dimension measures the degree of irregularity over multiple scales. It is a very often noninteger and it determines the difference between the fractal and Euclidean objects [8,10,11].

There are different methods to calculate FD such as walking divider method, box counting, and fractional Brownian motion [12]. Box-counting is the most straightforward method algorithm for computing FD of 1D and 2D objects [13-15]. It determines the fractal dimension of black and white digitized images of fractals. It works by covering fractal (its image) with boxes (squares) and then evaluating how many boxes are needed to cover fractal completely. Repeating this measurement with different sizes of boxes will result into the logarithmical function of box size (x-axis) and a number of boxes needed to cover fractal (y-axis). The slope of this function is referred to as the box dimension. Box dimension is taken as an appropriate approximation of fractal dimension [5,16].

Fractal analysis is commonly used in physics, image processing, and medical sciences [17]. Cancer research and medical images analysis are such examples for which fractal analysis has proved its utility [18-21]. The fractal-based techniques have been applied in many areas of digital image processing such as image segmentation, image analysis, image synthesis, computer graphics, and texture coding [22,23]. Based on the fractal theory, image context can be constructed by a set of model parameters which require fewer bits to describe than original image [5,24].

This research is aimed at calculating the different type of FD for erythrocytes in normal and abnormal states. Discriminant analysis using all measured parameters will be done. Predictor function will be extracted form discriminant analysis and will be evaluated to be used in erythrocytes classification.

Materials and Methods

Sample collection and preparation

Blood smear slides were collected from different medical laboratories. The slides were classified according to the erythrocytes abnormalities into three main groups: group 1: normal erythrocytes and were used as a control, group 2: echinocyte and group 3: sickle cells. One hundred slides from different volunteers were collected for each group. Thin blood smears were chosen for all groups since cell morphology and features were needed to be better preserved. Briefly, thin blood films were prepared by placing a drop of blood into the center of a slide and spread with the corner of another slide. By this

procedure, there was a region on the glass slide where the erythrocytes were homogeneously spread. The zone at which erythrocytes stop overlapping was chosen as the working area for microscopic analysis. All slides were left to air dry. In order to obtain good staining and presentation of cellular detail fixation with methanol was achieved. Increasing of the contrast of the blood smears was done by staining by Giemsa dilution. Ten shots were taken from a working area for each slide. The images were saved in TIFF format which is the best for post-processing as images were not compressed.

Imaging acquisition and images preprocessing

ImageJ2 open source software was used in image preprocessing [14]. The imaging system consisted of the compound light microscope attached to eyepiece camera. The eyepiece camera was connected to PC through USB. This system was enabled to capture the images directly from blood smear slides fixed on the stage of the microscope. All images were taken with magnification 40X and under the same conditions of illumination and resolution. All images were processed and analysed by Microscopic images were generated in RGB color format which is difficult to be segmented [25]. All images were converted to 8-bit grayscale. Then auto-correction of the brightness/contrast was done. This optimization was done based on the analysis of the image's histogram. The optimization was accomplished by allowing to some pixels in the image to be saturated to become black or white. Feature extraction and separation of images contents from the background and each other were done by image segmentation. Pixel unit scale was chosen to set all measurements. Optical density calibrated unit was chosen for peak evaluation and optical histogram.

Fractal dimension

HarFA open source software (Institute of Physical and Applied Chemistry, Brno University of Technology, Czech Republic) was used to perform factual analysis [26]. FD was measured by the box counting method. Erythrocytes image was covered with a grid, then counting of how many boxes cover a part of the image. The same procedure was done by using a smaller grid with a smaller box. Repeating this producer with a smaller and smaller grid and boxes, it ended up more accurately capturing the fine structure of the erythrocytes. FD was calculated as the gradient of the relationship of logN (Y-axis) against the value of log r (X-axis) [27].

$FD=log\ (N)/log\ (r) \rightarrow 1$

Where N is the number of boxes that cover the pattern and r is the magnification or the inverse of the box size. In HarFA a modification of traditional box counting enabled to compute three fractal dimensions FDBW, FDBBW, and FDWBW. FDBW is the fractal dimension which computes the surfaces perimeter of cells. FDBBW is the fractal dimension which computes the black border. FDWBW is the fractal demission which computes the white background. The three types of FD were used to build a discriminant model [28].

Statistical analysis

Form each image at least 50 erythrocytes were analysed. All the parameters were presented as mean ± SD. Comparing means was done by One-Way ANOVA. The covariance equality was evaluated by Box's test. The statistical significance was considered as $p<0.01$. FDBW, FDBBW, and FDWBW were used as a predictor variable to build a discriminant model [29]. The proposed discriminant analysis formed from the composition of canonical discriminant functions of a linear combination of independent predictor variables. Predicator functions (PF) were built by the coefficients of predictor variables which were the Fisher linear functions [29]. Casewise testing was performed to check the validity of PF. This was done by substitution of the predictor variables in PF. The largest PF indicates the group to which the erythrocyte was belonged to. IBM SPSS 23 was used to perform statistical analysis.

Results and Discussion

Figure 1 shows the images preprocessing and fractal analysis of erythrocytes. The fractal dimensions of the three groups are listed in Table 1. Also, Table 1 shows the results of ANOVA for means comparisons. It is clear that there is a significant difference between FDBW of normal group and the other two groups.

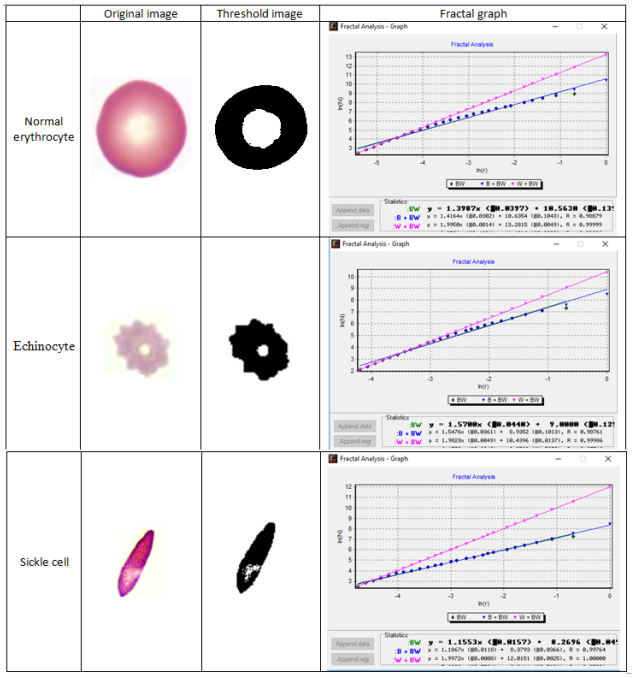

Figure 1. *Fractal analysis panel.*

Table 1. *Fractal dimensions of erythrocytes groups.*

Fractal dimension	Normal	Echinocyte	Sickle cell
FDBW	1.2997 ± 0.00705	1.4976 ± 0.02258	1.1015 ± 0.00702
FDBBW	1.4007 ± 0.01114	1.5076 ± 0.03135	1.1996 ± 0.00922

FDWBW	1.9008 ± 0.01414	1.9785 ± 0.03190	1.9892 ± 0.00787

*Data are represented as mean ± standard deviation **p<0.001

The difference between FDBBW of normal group and the sickle cell group was significant, and no difference was observed for the other group. No significant difference was found for FDWBW of normal and the other two groups. FDBW of echinocyte was 1.53 and higher than normal. In contrast, FDBW of sickle cells was 1.1 and lower than normal. The two canonical discriminant functions are shown in Table 2. Box's test for covariance equality was significant (P<0.001). The two discriminant functions are statistically significant (P<0.001). In consequence, according to the three groups of erythrocytes, fractal dimensions well-defined groups. A high value of the canonical correlation in the first (0.99) and second (0.9) discriminant functions indicate a high relationship between the group membership and discriminant function values. The bidimension space given by the two canonical discriminant functions is plotted in Figure 2. It shows the results correctly classified, indicating that 100% of the erythrocytes were correctly identified normal, 100% Echinocyte and 100% Sickle cell. The correlations between the canonical function and FDs are given in Table 3. Fisher's function coefficients are listed in Table 4. Those coefficients were used to build the PF equation as the following [28].

$$PF = FD_{BW} \times Coef_{FD_{BW}} + FD_{BBW} \times Coef_{FD_{BBW}} + FD_{WBW} \times Coef_{FD_{WBW}} + constant \rightarrow (2)$$

Where PF is the predictor function, FDBW is the fractal dimension which computes the surfaces perimeter of cells, $Coef_{FD_{BW}}$ is the group classification coefficient of FDBW, FDBBW is the fractal dimension which computes the black border, $Coef_{FD_{BBW}}$ is the group classification coefficient of FDBBW, FDWBW is the fractal demission which computes the white background, and $Coef_{FD_{WBW}}$ is the group classification coefficient of FDWBW. PF was used to classify erythrocytes. Classification procedure was done as follows: erythrocyte was chosen arbitrary from any slide diagnosed before. All steps for imaging processing were done. The measurements of FDBW, FDBBW, and FDWBW were performed. Three PF (PFNormal, PFEchinocyte, and PFSickle cell) were originated from the substitution for FDBW, FDBBW, and FDWBW and their coefficients given in Table 4 in Equation 2. PF with larger values indicted that erythrocyte was belonged to it.

Table 2. *Summary of the predictor functions.*

Function	Eigenvalue	% of variance	% cumulative	Canonical correlation
1	169.839[a]	97.4	97.4	0.997
2	4.590[a]	2.6	100.0	0.906

[a]First two canonical discriminant functions were used in the analysis.

Table 3. *Structure matrix of predictor model.*

	Function 1	Function 2
FDBW	0.874*	0.266
FDBBW	0.490*	-0.373
FDWBW	-0.024	0.883*

Pooled within-groups correlations between discriminating variables and standardized canonical discriminant functions variables ordered by absolute size of correlation within the function.

*Largest absolute correlation between each variable and any discriminant function

Table 4. *Classification function coefficients.*

	Normal	Echinocyte	Sickle cell
FD_{BW}	6215.496	7181.635	5237.724
FD_{BBW}	3360.137	3618.205	2853.382
FD_{WBW}	4265.718	4425.267	4502.541
(Constant)	-10447.534	-12483.521	-9075.426

*Fisher's linear discriminant functions

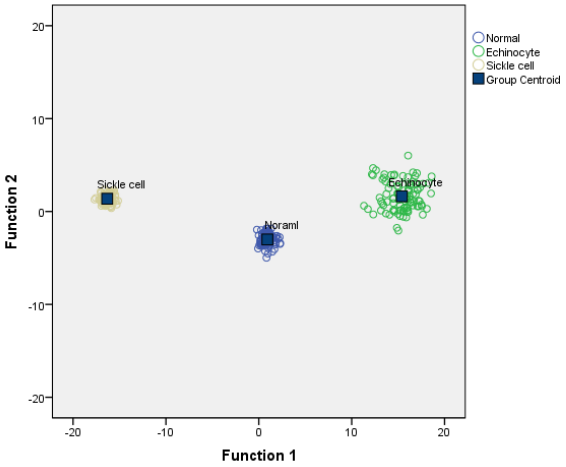

Figure 2. *Canonical discriminant functions.*

Automated cell morphometric method based on discriminant analysis was suggested by Albertini et al. [28]. Their model was based on the morphometric parameters such as chromogenic index and density profile extracted from the image processing of erythrocytes [28]. As mentioned before the discriminant analysis the most suitable for morphometric and morphological classification of erythrocytes [28,30]. The same analytical method was used in this study but with different predictor variables. Fractal analysis expresses well the details of the outer features of the object [31,32]. Consequently, fractal dimensions were chosen as predictor variables in the present study. FD was used before to study living cells and tissues in normal and different pathogenic

cases [31,33,34]. A set of fractal dimensions was examined to discriminant between three groups of erythrocytes. The discriminant analysis identifies the linear combinations of quantitative predictor variables that best characterize the differences between groups. Then the coefficients for each variable were estimated, and the resulting functions provide classification rule. By using FD from three different erythrocyte cell shape morphologies, three PF were constructed. PF sensitivity and specificity were higher than other classification functions used in the previous study. This can be explained as the fractal dimensions are more suitable to describe the morphological changes than other parameters.

Conclusion

The fractal analysis in the present study reflected well the morphological characteristics of the erythrocytes. Highly sensitive predictor model was constructed based on fractal dimensions. It can be concluded that fractal analysis is a powerful tool to describe the physical of biostructures. Also, it can be used as an accurate biomarker for cells differentiation.

Acknowledgment

The author would like to acknowledge the financial support of this work from the Deanship of Scientific Research (DSR), University of Tabuk (Tabuk, Saudi Arabia, under grant no. (S-1439-0133)).

References

1. Mandelbrot BB, Pignoni R. The fractal geometry of nature. WH Freeman New York 1983; 173.
2. Venkatalakshmi BAKT. Automatic red blood cell counting using Hough transform. 2013 IEEE Conference on Information and Communication Technologies (ICT) 2013.
3. Habibzadeh M, Krzyzak A, Fevens T. Comparative study of shape, intensity and texture features and support vector machine for white blood cell classification. J Theor Appl Comp Sci 2013; 7: 20-35.
4. Mohammed EA, Mohamed MM, Far BH, Naugler C. Peripheral blood smear image analysis: A comprehensive review. J Pathol Inform 2014; 5: 9.
5. Nonnenmacher TF, Baumann G, Barth A, Losa GA. Digital image analysis of self-similar cell profiles. Int J Biomed Comput 1994; 37: 131-138.
6. De Vico G, Peretti V, Losa GA. Fractal organization of feline oocyte cytoplasm. Eur J Histochem 2005; 49: 151-156.
7. Mandelbrot BB. The fractal geometry of nature. Updated Augm New York WH Freeman 1983; 468.
8. Weibel ER. Fractal geometry: a design principle for living organisms. Am J Physiol 1991; 261: 361-369.
9. Fuseler JW. Morphometric and fractal dimension analysis identifies early neoplastic changes in mammary epithelium of MMTV-cNeu mice. Anticancer Res 2014; 34: 1171-1177.
10. Sumelka W. Fractional calculus for continuum mechanics-anisotropic non-locality. Bull Polish Acad Sci Tech Sci 2016; 64: 361-372.
11. Zhang X, Xu Y, Jackson RL. An analysis of generated fractal and measured rough surfaces in regards to their multi-scale structure and fractal dimension. Tribol Int 2017; 105: 94-101.
12. Annadhason A. Methods of fractal dimension computation. Int J Comp Sci Inform Technol Secur 2012; 2.
13. Peng RD, Xie HP, Ju Y. Computation method of fractal dimension for 2-D digital image. J China Univ Mining Technol 2004; 33: 19-24.
14. Rueden CT, Schindelin J, Hiner MC, DeZonia BE, Walter AE, Arena ET, Eliceiri KW. ImageJ2: ImageJ for the next generation of scientific image data. BMC Bioinformatics 2017; 18: 529.
15. Nayak SR, Mishra J, Mohan Jena P. Fractal analysis of image sets using differential box counting techniques. Int J Inform Technol 2018; 10: 39-47.
16. Liebovitch LS, Toth T. A fast algorithm to determine fractal dimensions by box counting. Phys Lett A 1989; 141: 386-390.
17. Davies NA. Fractal dimension (df) as a new structural biomarker of clot microstructure in different stages of lung cancer. Thromb Haemost 2015; 114: 1251-1259.
18. Backes AR. Medical image retrieval and analysis by Markov random fields and multi-scale fractal dimension. Phys Med Biol 2015; 60: 1125-1139.
19. Ali Z. Detection of voice pathology using fractal dimension in a multiresolution analysis of normal and disordered speech signals. J Med Syst 2016; 40: 20.
20. Mohan G, Subashini MM. MRI based medical image analysis: survey on brain tumor grade classification. Biomed Sig Proc Control 2018; 39: 139-161.
21. Bitler A, Dover RS, Shai Y. Fractal properties of cell surface structures: A view from AFM. Semin Cell Dev Biol 2018; 73: 64-70.
22. Landini G. Fractals in microscopy. J Microsc 2011; 241: 1-8.
23. Yao B. Multifractal analysis of image profiles for the characterization and detection of defects in additive manufacturing. J Manufact Sci Eng 2018; 140: 031014.
24. Harrar K. Oriented fractal analysis for improved bone microarchitecture characterization. Biomed Sig Proc Control 2018; 39: 474-485.
25. Markiewicz T. Thresholding techniques for segmentation of atherosclerotic plaque and lumen areas in vascular arteries. Bull Polish Acad Sci Tech Sci 2015; 63: 269-280.
26. Zmeskal O. Fractal analysis of image structures. Harmon Fract Image Anal 2001; 3-5.
27. Karperien A. FracLac for ImageJ http://rsb. info. nih. gov/ij/plugins/fraclac/FLHelp. Introduction. html 1999.
28. Albertini MC. Automated analysis of morphometric parameters for accurate definition of erythrocyte cell

shape. Cytometry Part A J Int Soc Analyt Cytol 2003; 52: 12-18.

29. Anderson MJ. A new method for non-parametric multivariate analysis of variance. Austral Ecol 2001; 26: 32-46.
30. Eldibany MM. Usefulness of certain red blood cell indices in diagnosing and differentiating thalassemia trait from iron-deficiency anemia. Am J Clin Pathol 1999; 111: 676-682.
31. Stankovic M. Quantification of structural changes in acute inflammation by fractal dimension, angular second moment and correlation. J Microsc 2016; 261: 277-284.
32. Pribic J. Fractal dimension and lacunarity of tumor microscopic images as prognostic indicators of clinical outcome in early breast cancer. Biomark Med 2015; 9: 1279-1287.
33. Revin VV. Study of erythrocyte indices, erythrocyte morphometric indicators, and oxygen-binding properties of hemoglobin hematoporphyrin patients with cardiovascular diseases. Adv Hematol 2017; 2017.
34. Smits FM, Porcaro C, Cottone C, Cancelli A, Rossini PM, Tecchio F. Electroencephalographic fractal dimension in healthy ageing and alzheimers disease. PLoS One 2016; 11: e0149587.

*Correspondence to

Mohamed A. Elblbesy

Department of Medical Laboratory Technology

University of Tabuk

Saudi Arabia